OPEN ACCESS

Saudi Journal of Civil Engineering

Abbreviated Key Title: Saudi J Civ Eng
ISSN 2523-2657 (Print) |ISSN 2523-2231 (Online)
Scholars Middle East Publishers, Dubai, United Arab Emirates
Journal homepage: https://saudijournals.com/journal/sjce/home

Original Research Article

Microstructure Characteristics, Mechanical and Corrosion Properties of Copper Alloyed Hypo-Eutectic Grey Cast Iron

Kutelu, Bolarinwa Johnson[1], OGUNDEJI Francis Oladapo[1*], Oke Olugbenga[1]

[1]Department of Mineral and Petroleum Engineering Technology, the Federal Polytechnic, Ado-Ekiti, Ekiti, State, Nigeria

DOI: 10.36348/sjce.2023.v07i10.002 | **Received:** 09.09.2023 | **Accepted:** 14.10.2023 | **Published:** 05.11.2023

***Corresponding author:** OGUNDEJI Francis Oladapo
Department of Mineral and Petroleum Engineering Technology, the Federal Polytechnic, Ado-Ekiti, Ekiti, State, Nigeria

Abstract

In this study, influence of varied copper addition on the mechanical properties and corrosion characteristics of grey cast iron (GCI) was investigated. As-cast unalloyed and 0.035 wt. %, 0.65 wt. % 0.85 wt. % and 1.18 wt. % copper alloyed GCI samples were produced using rotary furnace. Chemical compositions of the samples were determined by Optical Emission Spectroscopy using ARL QuantoDeskSpectro analysis machine. Tensile and hardness measurements were made using INSTRON tensile testing machine- model 3369 and Universal Rockwell hardness testenr- model 8187LKV respectively. Samples' characterization was done using Philips SEM (XL30 TMP). And electrochemical measurement was determined using AUTOLAB PGSTAT 204N instrument. From the results, the as-cast unalloyed, 0.035 wt. % and 0.85 wt. % and 1.18 wt. % Cu alloyed GCI samples revealed lamella graphite in pearlite matrix, short flake graphite in pearlitic-ferrritic matrix, Type A flake graphite in pearlitic-ferritic matrix and long flake graphite in ferritic-pearlitic matrix respectively. Tensile, hardness and elongation properties of the copper GCI samples ranked superior over the as-cast unalloyed GCI sample. Optimum tensile value 158.26 N/mm^2 and hardness value 447.4 HRC were revealed by the 0.85 wt. % Cu, and optimum ductility value of 2.79% was revealed by the 1.18 wt. % Cu alloyed GCI sample. In general, copper alloyed GCI samples showed better corrosion resistance relative to the as-cast unalloyed GCI sample. The copper alloyed GCI samples showed better corrosion resistance relative as compared to the as-cast unalloyed GCI sample. Least corrosion rate of 0.0011297 mm/yr with polarization resistance of 174.58 Ω was revealed by the 0.85 wt. % Cu alloyed GCI sample. Hence, it is most suitable in application requiring high to moderate strength is marine environment.

Keywords: Copper addition, corrosion, lamella graphite, flake graphite, perriti matrix perritic-ferritic matrix, ferriti-pearlitic matrix.

INTRODUCTION

Grey cast iron (GCI) is comprised mainly of iron and carbon, which range from 2.5 to 4%, silicon, which range from 1% to 3%, manganese, which range from 0.1% t01.2% and other alloying elements, which are present in trace quantities (Krause, 2012; Hsu and Lin, 2011). Generally, GCI is characterized by either pearlitic, ferritic, ferrritic- pearlitic and pearlitic- ferritic matrix (Collini *et al.*, 2008). However, matrix of the as-cast microstructure is pearlitic with finely distributed graphite slamell as (Pluphrach, 2010).

GCI has a number of unique properties such as good castability and damping capacity, moderate wear resistance and moderate corrosion resistance, high thermal conductivity and higher strength in compression than in tension (Sheriff *et al.*, 2019; Seidu, 2014; Agunsoye *et al.*, 2014; Sherrif;). Also, its excellent machinability has been traced to the flake-like structure in its matrix (Vadiraj and Tiwari, 2014; Adedayo, 2013). Casting of GCI have been widely utilized in pressure applications such as cylinder blocks, manifolds, pipe fitting, compressors (Pluphrach, 2010). Other areas of applications included structural components in the wind power industry, blocks, break pad kit, engine blocks, shafts, electric motor, pipes, machine bases and cook wares manifolds, pipe fittings, compressors, pumps (Bates, 1997). Based on ASTM A 247, flake graphite can be grouped into Type A, B, C and D, these flake graphite act as stress concentrators and, in consequence, poor toughness and elastic behavior GCI (Collini *et al*., 2008).

It can therefore be said that mechanical properties of the grey castiron are controlled by flake graphite.

Industrial casting practice have been used to improve performance integrity of GCI, Vadiraj and Tiwari, (2014) improved on the wear characteristic of grey cast iron by silicon addition. Copper addition to grey cast iron melt was used to stabilize pearlite, coarsen graphite, increase the number of eutectic cells and reduce eutectic cell size (Agunsoye *et al.*, 2014). With the presence of 99% pure Cu in the grey cast iron melt, inhibition of cementite formation was achieved in a developed alloy of cast iron and copper (Fe-Cu) using stir cast process (Johnson *et al.*, 2014).

Today, GCI has become a versatile cast metal material for modern industrial manufacturing in place of steel. As a result, there have been extensive research efforts on mechanical properties of copper alloyed GCI in the recent. However, the same cannot be said of corrosion property. Yet, GCI is utilized in applications requiring corrosive environment such as underground pipes. In this work, mechanical properties as well as corrosion characteristics of copper alloyed GCI in marine environment were considered.

2. METHODOLOGY

2.1 MATERIALS

The materials used for the work included auto parts scrap, graphite, limestone, copper wire, cylindrical bar wooden material with dimension 190.5 mm long and 25 mm diameter. The elemental composition of the auto parts scrap is shown in Table 1. It was obtained using Optical Emission Spectroscopy (OES) testing machine (ARL Quanto Desk Spectro).

Table 1: Elemental composition of the automobile scrap

%C 3.97	**%Si 1.94**	**%Mn 0.87**	**%P 0.088**	**%S 0.131**	**%Cr 0.163**	**%Ni 0.058**	**%Mo 0.0015**
%Al 0.0058	%Cu 0.137	%Co 0.015	%Ti 0.0015	%Nb <0.0025	%V 0.0099	%W <0.010	%Pb 0.0083
%Mg 0.0033	%B <0.0005	%Sn 0.0083	%Zn 0.0081	%As 0.020	%Bi <0.0015	%Ce <0.0030	%Zr <0.0015
%La <0.0033	%Fe 92.5						

2.2 METHODS

2.2.1 Production of Grey Cast Iron

The scrap auto parts were broken down by hitting with sledge hammer into smaller sizes that can freely pass through the charging sprout of the rotary furnace, and later weighed with a weighing balance. The rotary furnace was preheated for an hour before charging. 50Kg cast iron auto scraps, 2Kg graphite and 1Kg limestone were charged into the furnace and heated until melting occurred. The rotary furnace was heated to 1,485°C for 15 hours, at this temperature and time; the charges had become melted completely and ready for tapping. Ladle was preheated to receive the melt during tapping. Ferrosilicon (FeSi) inoculant with 78% Si, 0.21% Al, Fe-bal. with particle size 0.5mm was added to the metal stream during tapping from rotary furnace to ladle at 1,470^{o}C, and the tapping time was 15sec. The first melt, which Serves as the control was not copper alloyed, while the second, third and fourth melts were alloyed with 0.035 wt. %Cu, 0.85 wt. %Cu and 1.18 wt. %Cu respectively. The slag float on top of the melt was removed with the aid of a mild steel rod before pouring to prevent slag inclusions in the casting. The melt was poured at 1,450^{o}C temperature into the mold through the funnel-shaped cut impression and passes through the sprue, runner, and runs through the gate to fill the mold cavity until it rose up to the riser, and the pouring time lasted for 10sec. Thereafter, it was knocked out after the melt had completely solidified.

2.2.2 Chemical Analysis

The chemical compositions of the castings (as-cast unalloyed and the copper alloyed GCI samples) were examined using Optical Emission spectroscopic (OES) testing machine (ARL Quanto Desk Spectro).

2.4 Microstructure

Surfaces of the samples were ground using laboratory grinding machine with sets of emery papers of the grades 60, 120, 240, 320, 400, 800 and 1200 microns. As the emery papers were changed from one to the other, the samples were turned through an angle of 90 so as to remove the scratches sustained from the previous grinding until a scratch-free surface is obtained. After grinding, the samples were polished using laboratory polishing machine to give a mirror-like surface using billiard cloth. The billiard cloth consists of abrasive particles that are not firmly fixed but suspended in a liquid among the fibres of the cloth. Diamond paste of different microns (6m,3m,1m) were applied on the billiard cloth and the samples were polished by holding it with less pressure against the rotating disc until a mirror-like surface is obtained. Philips SEM (XL30 TMP) was used to characterize the samples.

2.5 Mechanical Testing

2.5.1 Tensile

Samples used for the tensile test were prepared in accordance with ASTM E 8-04. They were machined to 3.5 mm diameter (⌀) and 32 mm gauge length (L) (Fig.). INSTRON tensile testing machine, model 3369

was used; load was applied at the rate of 0.5mm/min till fracture, after which tensile strength and percentage elongation were taken.

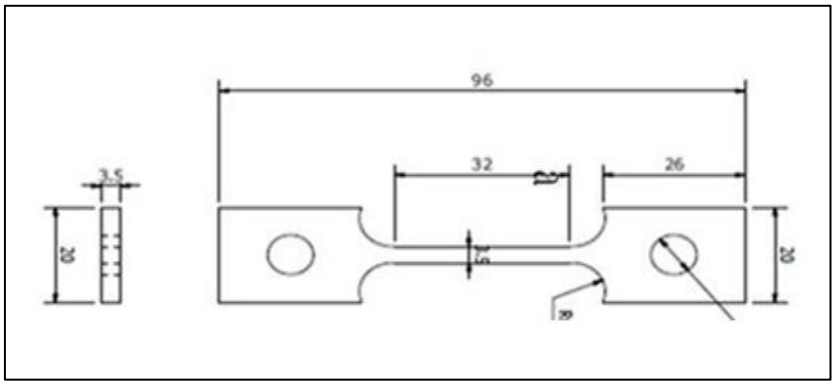

Fig. 1: Tensiletestspecimen

2.5 Hardness Measurement

Hardness specimens with dimension 20 mm length, 20 mm breadth and 4.5 mm thickness (Fig.2) were prepared in accordance with ASTM E 8-04 standard. Universal Rockwell hardness tester model 8187LKV was used. The specimen was placed on the anvil and moved up until it came in contact with the Diamond cone indenter, the dial gauge was set to zero using minor load of 10kgf. Thereafter, major load of 150kgf was applied on the specimen, and the corresponding hardness value was measured on the C-scale. Three indentations were made with gap of about 3 mm in- between and the average value was recorded.

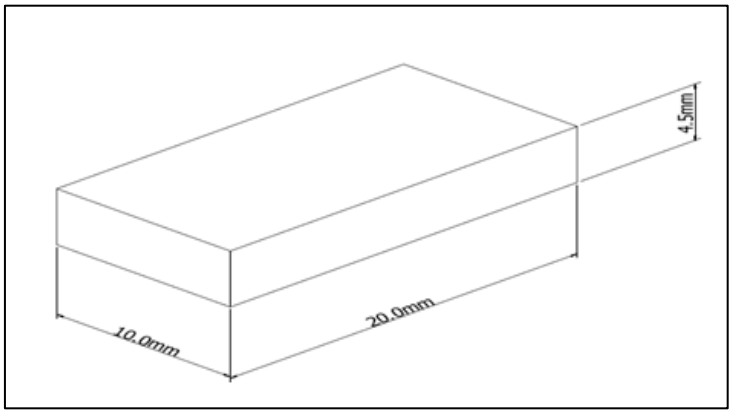

Fig. 2: Hardnesstestspecimen

2.5 Corrosion Test

The electrochemical experiments were carried out using AUTOLAB PGSTAT 204N instrument, piloted by NOVA software. The experiments were performed according to ASTM G3-14 (American Society for Testing & Materials G3-14, 2014) at room temperature using a three-electrode corrosion cell setup. Saturated silver/silver chloride as reference electrode, platinum rod is the counter electrode and the unalloyed as-cast GCI and copper alloyed GCI are the working electrode. The working was immersed in a test solution for 30 min until a stable open circuit potential was attained. Potentio dynamic polarization measurements were carried out at a scan rate of 1.0 mV/s at a potential initiated at −250 to +250 mV. After each experiment, the electrolyte and the test sample was replaced. All corrosion potential measurements recorded in this study were with respect to the saturated calomel electrode.

3. RESULTS AND DISCUSSION

3.1 Chemical Analysis

Table 2 depictsresults of chemical analysis of the as castunalloyed and copper alloyed GCI samples. Based on the carbon equivalent (CE) values, the samples are hypoeutectic grey cast iron (Sheriff *et al.*, 2019). Solidification of melts into either cementite or graphite is determined by the presence of certain alloying elements), Si, Cu and Al are graphite promoters and Cr, V and Mn carbide promoters (Sheriff *et al*., 2019; Swain and Sen, 2009). Si and MN contents of the samples ranged within ASTM A536 standard.

Table 2: Chemical analysis of the grey cast iron samples

Grey Cast Iron	Chemical Composition wt.%						CE (wt. %)	Mn/S	(Mn)x (S)
	C	Si	Mn	P	S	Al			
U.I.	3.08	2.45	0.234	0.088	0.135	0.0010	3.15	1.73	0.032
0.035wt. %Cu	3.01	2.93	0.220	0.069	0.143	0.0076	3.10	1.54	0.031
0.85wt. %Cu	3.10	2.98	0.201	0.060	0.140	0.0087	3.08	1.43	0.028
1.18wt%Cu	3.03	2.98	0.101	0.071	0.149	0.0098	3.17	0.68	0.015

3.2 Microstructure Analysis

From the SEM micrographs in Plates 1, 2, 3 and 4, the samples reveal variations in size, distribution, shape and interconnectivity of graphite. Microstructure of the as-cast unalloyed GCI sample (Plate 1) is characterized by a number of long graphite flakes, which are sparsely distributed within presumed ferrite matrix. Microstructure of the GCI sample with 0.035 wt. %. Cu (Plate 2) is comprised of fine and short graphite flakes, which are uniformly distributed within ferrite-pearlite matrix. Microstructure of grey iron with 0.85 wt. % Cu (Plate 3) is comprised of Type A graphite flakes, which are uniformly distributed within pearlite- ferrite matrix (ASTM A247, 2006). Short graphite flakes length of 0.85 wt. %. Cu alloyed GCI sample relative to0.035 wt. % Cu alloyed GCI sample is attributable to rapid graphitization that resulted from increased addition of copper of the former (Agunsoye *et al*., 2014).

Microstructure of the 1.18 wt. %. Cu alloyed GCI sample (Plate 4) is comprised of fine graphite flakes, which are uniformly distributed within presumed ferrite-pearlite matrix. With increased copper addition, rapid graphitizing is favored, growth and nucleation rates of graphite were increased, leading to more ferrite phase (Agunsoye *et al*., 2014; Gourahari and Soumya, 2012).

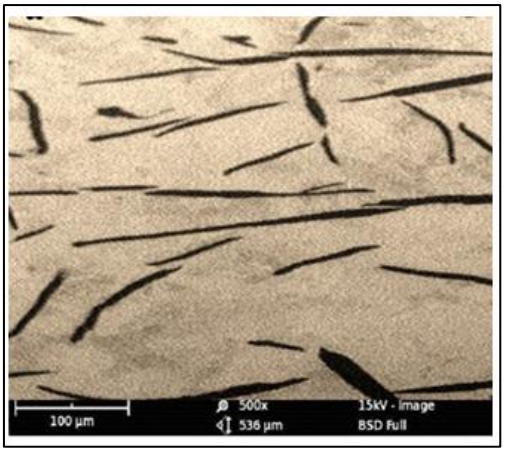

Plate 1: SEM Micrograph of unalloyed as-cast hypo-eutectic grey cast iron

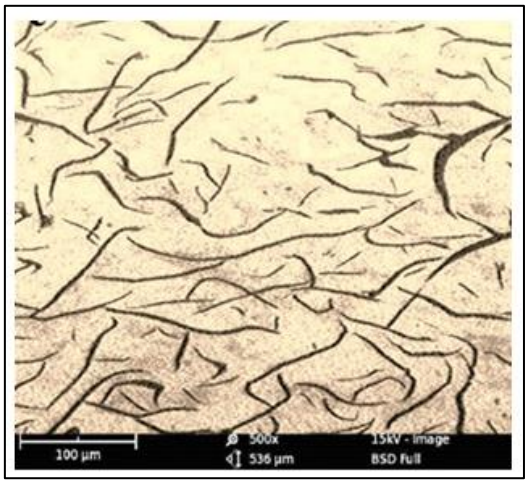

Plate 2: SEM Micrograph of 0. 65wt. % Cu alloyed hypo-eutectic grey cast iron

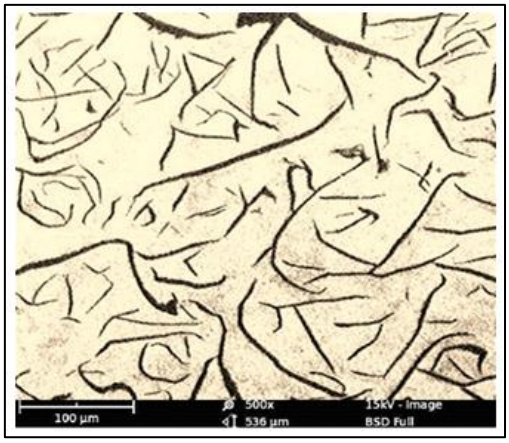

Plate 3: SEM Micrograph of 0.85wt. % Cu alloyed hypo eutectic grey cast iron

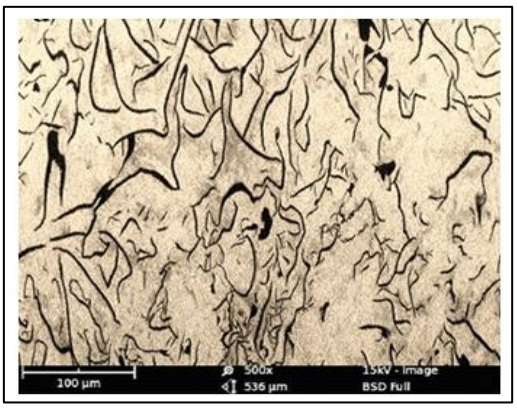

Plate 4: SEM Micrograph of 1.18wt. % Cu alloyed hypo eutectic grey cast iron

3.2 Mechanical properties

The superior tensile strength of the Cu alloyed GCI samples as compared to the as-cast unalloyed GCI sample (Fig.3) resulted from the presence of pearlite. Copper is a strong graphitizer, it promotes the formation of pearlite and strengthens the pearlite formed (Das *et al*., 2013; Hsu and Lin, 2011). The optimum tensile strength revealed by 0.85 wt. %Cu alloyed GCI sample is attributed to increased presence of pearlite that resulted from more graphitization with concomitant more strengthening of the formed pearlite (Johnson *et al*., 2013; Srinivasan and Kondic, 1975).

The subsequent reduction in tensile strength with increasing addition of copper shown by 1.185 wt. %Cu GCI sample was due to more volume fraction of ferrite that resulted from decomposition of pearlite to ferrite and carbon (Pluphrach, 2010; Collini *et al*., 2008; Srinivasan, and Kondic, 1975). Also, the presence of crack at the tip of the resulted long graphite flakes was palpable, which could have led to crack propagation through the microstructure (Hsu and Lin, 2011; Mohebbi, 2009).

Hardness of austempered ductile iron (ADI) was reported to increase with increasing copper addition due to short graphite flake that resulted from strengthening of the pearlite phase (Seidu, 2014; Das *et al*., 2013). The superior hardness property of the copper alloyed GCI samples relative to the as-cast unalloyed GCI sample (Fig. 4) is in congruent with the findings of the earlier researchers. Copper increases graphitization, promotes, refines and stabilizes pearlite, these effects on pearlite with its solid solution strengthening of ferrite could have accounted for the improved and optimum hardness of 0.035 wt. %Cu alloyed GCI sample and 0.85 wt. %Cu alloyed GCI sample respectively. And decrease in hardness value of the 1.18 wt. % GCI sample relative to 0.85 wt. % GCI sample was accounted for by increased presence of ferrite phase (Pluphrach, 2010; Collini *et al*., 2008; Srinivasan, and Kondic, 1975).

In converse to pearlite, ferrite is relatively soft and hence, characterized by more ductility and elongation (ZouandNakea,2014; Srinivasan and Kondic, 1975). Therefore, the superior elongation property of 1.18 wt. %Cu GCI sample as compared to 0.035wt. % Cu, as-cast unalloyed and 0.85 wt. %Cu GCI samples correspondingly (Fig. 5) may be hinged on increased volume fraction of ferrite.

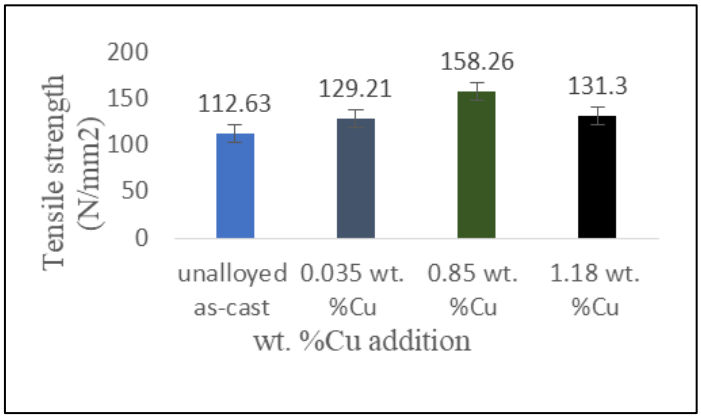

Fig. 3: Tensile property of the as-cast unalloyed and copper alloyed GCI sample

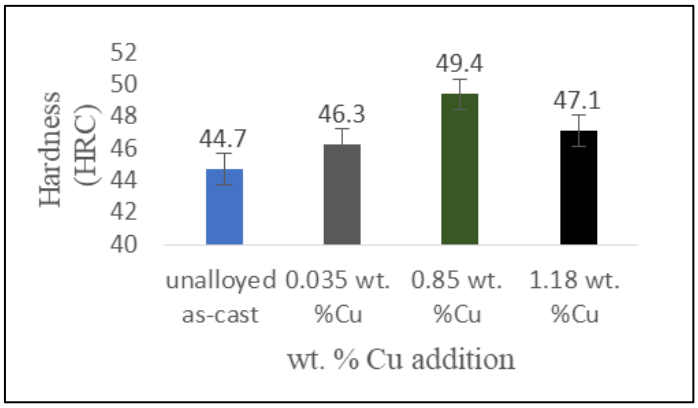

Fig. 4: Hardness property of the as-cast unalloyed and copper alloyed GCI sample

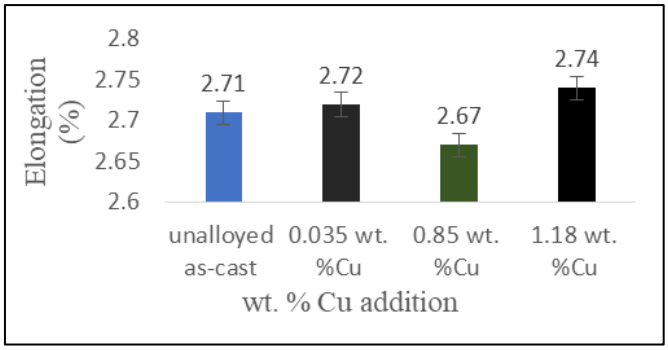

Fig. 5: Elongation property of the as-cast unalloyed andcopper alloyed GCI sample

3.3 Corrosion Characteristics

Electrochemical corrosion data of the as-cast unalloyed GCI sample and copper alloyed GCI samples in 1M NaCl environment is presented in Table 3. Fig. 6 depicts polarization curves of the corroding samples. There sulting varied size and shape of graphite flakes, and distribution within ferritic matrix, ferritic-pearlitic matrix, pearlitic ferritic matrix and ferric-pearlic matrin for the as-cast unalloyed GCI sample, 0.035 wt. % Cu alloyed GCI sample,0.85 wt. % Cu alloyed GCI sample and1.18 wt. % Cu alloyed GCI sample respectively, accounted for variations in the corrosion characteristic of the samples (Sohail *et al.*, 2019; Linar, 2018; Lunarska, 1996).

Ferrite structure is least resistant to corrosion relative to pearlite structure (Asifal *et al.*, 2019; Sohail *et al.*, 2019). Ruscak and Perng, 1995). The as- cast unalloyed GCI sample, lacking in copper and characterized by long graphite flake in ferrite matrix revealed least polarization resistance, and hence highest corrosion rate in the studied environment as compared to 0.035 wt. % Cu, and 1.18 wt. % Cu and 0.85 wt. % Cu alloyed GCI samples correspondingly.

Table 3: Electrochemical corrosion data of specimens in 1M in NaCl environment

Sample description	*Ecorr* (V)	*i corr*(A/cm^2)	Corrosion rate (mm/yr)	Polarization Resistance (Ω)
Unalloyed as cast	-453.042	1.206	0.014004	138.19
0.035 wt.% Cu	-423.326	0.2065	0.002396	150.54
0.85 wt.% Cu	-416.805	0.09736	0.0011297	174.58
1.18 wt.% Cu	-421.034	0.1901	0.01220	143.74

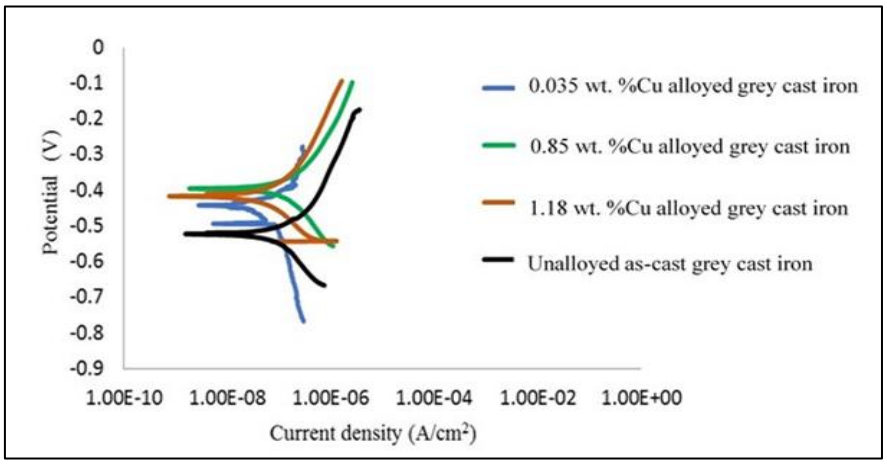

Fig. 6: Potentiodynamic polarization curves of specimens in 1M NaCl environment

4. CONCLUSIONS

From the results of the research, the following conclusions were drawn:

1. Generally, graphite morphology, mechanical property and corrosion characteristics of the grey cast iron is influenced by the copper addition.
2. The as-cast unalloyed revealed lamella graphite in pearlite matrix, the 0.035 wt. % Cu alloyed sample showed short flake graphite in pearlitic-ferritic matrix, the 0.85 wt. % Cu alloyed sample showed Type A flake graphite in pearlitic-ferritic matrix and 1.18 wt. % Cu alloyed GCI samples revealed long flake graphite in ferritic-pearlitic matrix.
3. Tensile, hardness and elongation properties of

the copper GCI samples ranked superior over the as-cast unalloyed GCI sample.

4. Optimum tensile value 158.26 N/mm^2 and hardness value 447.4 HRC were revealed by the 0.85 wt. % Cu, and optimum ductility value of 2.79% was revealed by the 1.18 wt. % Cu alloyed GCI sample.
5. The copper alloyed GCI samples showed better corrosion resistance relative to the as-cast unalloyed GCI sample. And the least corrosion rate of 0.0011297 mm/yr with polarization resistance of 174.58 Ω was shown by the 0.85 wt. % Cu alloyed GCI sample.

REFERENCES

- Adedayo, A. V. (2013). Relationship between graphite flake sizes and the mechanical properties of grey iron. *International Journal of Materials Science and Applications*, *2*(3), 94-98. doi:10.11648/j.ijmsa.20130203.14x.
- Agunsoye, J. O., Bello, S. A., Hassan, S. B., Adeyemo, R. G., & Odii, J. M. (2014). The effect of copper addition on the mechanical and wear properties of grey cast iron. *Journal of Minerals and Materials Characterization and Engineering*, *2*(05), 470.
- Asifal, H. S., Amit, S., Jitendra, K. S., Sohail, M. A. K., Nabeel, A., & Manojit. G. (2019). Corrosion characteristics of copper aided austempered grey cast iron. *Material*, pp.1-18,wwwmdpi.com/journal/material
- ASTM A247. (2006). Standard test method for evaluating the microstructure of graphite in iron castings. *ASTM International*, 100 Barr Harbor Drive, West Conshohocken, pp19428-2959 USA.
- Bates, C. E. (1984). Effects of Alloy Elements on the Strength and Microstructure of Gray Cast Iron.(Retroactive Coverage). *Transactions of the American Foundrymen's Society.*, *92*, 923-946.
- Collini, L., Nicoletto, G., & Konečná, R. J. M. S. (2008). Microstructure and mechanical properties of pearlitic gray cast iron. *Materials Science and Engineering: A*, *488*(1-2), 529-539.
- Das, A. K., Dhal, J. P., Panda, R. K., Mishra, S. C., & Sen, S. (2013). Effect of alloyingelements and processing parameters on mechanical properties of austemperedductile iron. *Journal of Material sand Metallurgical Engineering*, *3*(1), 8-16.
- Gourahari, B., & Soumya, R. S. (2012). Effect of Copper on the Properties of Austempered Ductile Iron Castings. *A Thesis for Bachelor of Technology Submitted to Department of Metallurgical and Materials Engineering, National Institute of Technology, Roukella*.
- Hsu, C. H., & Lin, K. T. (2011). A study on microstructure and toughness of copper alloyed and austempered ductile irons. *Materials Science and Engineering: A*, *528*(18), 5706-5712. doi:10.1016/j.msea.2011.04.035
- Johnson, O. A., Sefiu, A. B., Bolaji, H., & Adeyemo, R. G. (2014). The Effect of copper addition on the mechanical and wear properties of grey cast iron, Journal of Minerals and Materials Characterization and Engineering *2*(5), 470-483.
- Krause, D. E. (2012). Gray Iron- A unique engineering material. Gray, Ductile and Malleable Iron Castings – Current Capabilities, ASTM STP 455, *American Society for Testing and Materials*, Philadelphia, 3-28.
- Linar, F. K. (2018). The corrosion behaviour and wear resistance of grey cast iron. *Kofa Journal of Engineering*, 1, 118-132.
- Lunarska, E. (1996). Effect of graphite shape on the corrosion of grey cast iron in phosphoric acid. *Materials and Corrosion*, *47*(10), 539-544. View at: Google Scholar
- Mohebbi, H. (2009). Characterisation of the fatigue properties of cast irons used in the water industry and the effect on pipe strength and performance," in *Proceedings of the 7th International Conference on Modern Practice in Stress and Vibration Analysis*, IOP Publishing, Cambridge, UK, September 2009.View at: Google Scholar
- Pevec, M., Oder, G., Potrč, I., & Šraml, M. (2014). Elevated temperature low cycle fatigue of grey cast iron used for automotive brake discs. *Engineering Failure Analysis*, *42*, 221-230. doi:http://dx.doi.org/10.1016/j.engfailanal.2014.03.021
- Pluphrach, G. (2010). Study of the effect of solidification on graphite flakes microstructure and mechanical properties of an ASTM a-48 gray cast iron using steel molds. *Sonklanakarin Journal of Science and Technology*, *32*(6), 613.
- Ruscak, M., & Perng, T. P. (1995). Effect of ferrite on corrosion of Fe-Mn-Al alloys in sodium-chloride solution, *Corrosion*, *51*, (10), 738–743, View at: Google Scholar
- Seidu, S. O. (2014). Effect of compositional changes on the mechanical behaviour of grey cast iron. *Journal of Metallurgical Engineering (ME) Volume*, *3*(2).
- Sherrif, O. S., Saliu, O. S., Taiwo, S. A., & Lulian, R. (2019). Chilling effect of iron powder on the microstructure and hardness property of strongly hypereutectic grey cast iron, ANNALS of Faculty Engineering Hunedaora- *International Journal of Engineering*, *4*, 13-22.
- Sohail, H. S., M. A. K., Nabeel, A., & Manojit, G. (2019). Corrosion characteristic of copper-aided austempered gray cast iron (AGCI), Material, wwwmdpi.com/jounal/material.
- Srinivasan, M. N., & Kondic, V. (1975). Relating microstructure to mechanical properties of flake cast iron, in *Proceedings of the International Symposium on the Metallurgy of Cast Iron*, Georgi Publishing Company, Geneva, Switzerland, View at: Google Scholar

- Tel'manova, O. N., Karyazin, P. P., & Shtanko, V. M. (2012). Behavior of cast-iron with lamellar and globular graphite in dilute acids, *Protection of Metals*, 16(1), 45-47.
- Vadiraj, A., Tiwari, S. (2014). Effect of silicon on mechanical and wear properties of alloyed grey cast iron. *J Mater Eng perform, 23*, 3001-3006.
- Zou, Y., & Nakea, H. (2014). Influenceofboron onferrite formationincopperaddedspheroidal graphitecast iron.*Journalof China Foundry*, *11*(4), 375-381.